

Santiago Sosa

Articulo

-  Thesis
-  RedesT3
-  PUCE ESMERALDAS MOODLE

Detalles del documento

Identificador de la entrega

trn:oid:::1:3479194356

Fecha de entrega

11 feb 2026, 3:52 p.m. GMT-5

Fecha de descarga

11 feb 2026, 4:03 p.m. GMT-5

Nombre del archivo

template.pdf

Tamaño del archivo

33.9 MB

18 páginas

7448 palabras

41.337 caracteres

36 % detectado como IA

El porcentaje indica la cantidad combinada del texto generado probablemente con IA, así como el texto generado con IA que también se parafaseó probablemente con IA.

Precaución: Se necesita revisión.

Es esencial comprender los límites de la detección de IA antes de tomar decisiones acerca del trabajo del estudiante. Te alentamos a obtener más información acerca de las funciones de detección de IA de Turnitin antes de usar la herramienta.

Grupos de detección

25 Sólo generado con IA 36%

Texto generado probablemente con IA desde un modelo de lenguaje de gran tamaño.

0 Texto generado con IA que se parafaseó con IA 0%

Texto generado probablemente con IA que se revisó probablemente usando una herramienta de paráfraseo de IA o de reescritura.

Aviso legal

Nuestra evaluación de escritura con IA está diseñada para ayudar a los académicos a identificar texto que podrían haberse preparado mediante una herramienta de IA generativa. Es posible que nuestra evaluación de escritura con IA no siempre sea precisa (por ejemplo, nuestros modelos de IA pueden producir tanto resultados falsos positivos como falsos negativos), por lo que no debe usarse como único fundamento para aplicar sanciones a un estudiante. Para determinar si es un caso de deshonestidad académica, se necesita de un escrutinio mayor y el juicio humano, junto con la aplicación de las políticas académicas específicas de la organización.

Preguntas frecuentes

¿Cómo debería interpretar los falsos positivos y el porcentaje de escritura con IA de Turnitin?

El porcentaje que se muestra en el reporte de escritura con IA es la cantidad del texto calificado en la entrega que el modelo de detección de escritura con IA de Turnitin determina se generó probablemente con IA desde un modelo de lenguaje de gran tamaño, o se generó probablemente con IA y es probable que se haya revisado usando una herramienta de paráfraseo de IA o una herramienta aleatoria de palabras.

Los falsos positivos (que marcan incorrectamente alertas de texto escrito por humanos como generado con IA) son una posibilidad en los modelos de IA.

Los puntajes de detección de IA inferiores al 20 %, que no aparecen en reportes nuevos, tienen una mayor probabilidad de ser falsos positivos. Para reducir la probabilidad de malinterpretación, no se atribuye ningún puntaje o resultado y se indican con un asterisco (*%).

El porcentaje de escritura con IA no debe ser el único fundamento para determinar si ha ocurrido una mala conducta. El revisor/instructor debería usar el porcentaje como un medio para iniciar una conversación formativa con sus estudiantes o usarlo para examinar el ejercicio entregado según las políticas de la escuela.

¿Qué significa 'texto calificado'?

Nuestro modelo sólo procesa texto calificado en la forma de escritura de formato largo. La escritura de formato largo significa que los enunciados individuales en párrafos que constituyen una parte más grande del trabajo escrito, como un ensayo, una tesis, un artículo, etc. El texto calificado que se ha determinado que se generó probablemente con IA se resaltará en color cian en la entrega, y el texto generado probablemente con IA y luego paráfraseado probablemente con IA se resaltará en color morado.

El texto no calificado, como viñetas, bibliografías comentadas, etc., no se procesará y puede crear disparidad entre los puntos destacados de la entrega y el porcentaje mostrado.



Article

Physics Laboratory Implementation for Engineering through Retrofitting with IoT Technologies in a Hybrid Learning Environment.

Walter Santiago Sosa Mejía

Pontificia Universidad Católica del Ecuador, Sede Esmeraldas; wssosa@pucese.edu.ec

Abstract

The modernization of physics laboratories in resource-limited contexts presents significant challenges. This article presents the design and validation of a remote laboratory system for the study of Uniformly Accelerated Rectilinear Motion (UARM), implemented through an Internet of Things (IoT) retrofitting strategy on pre-existing equipment. The proposed architecture utilizes an ESP32 microcontroller, hereafter referred to as the control module, and infrared sensors for data capture, managed through a web interface that allows for real-time control and visualization. To validate the system, a comparative study was conducted with 140 trials (70 in remote mode and 70 in presencial mode). Results demonstrate that the remote prototype achieves kinematic precision comparable to the traditional setup, maintaining high stability in measurements of time, velocity, and acceleration, with controlled standard deviations. It is concluded that the IoT retrofitting methodology is a viable and scalable solution to democratize access to high-quality experimental education in hybrid environments, without requiring large infrastructure investments.

Keywords: Retrofitting; Internet of Things; Remote laboratories; UARM; Low-cost instrumentation; Cloud services; Engineering education

1. Introduction

Physics laboratories constitute an essential component for the experimental verification of laws and models, as well as for the validation of measurement and control systems. Traditionally, these environments have operated strictly in a face-to-face manner, with analog or digital instrumentation requiring the user's physical presence in the laboratory. However, the increasing digitization of scientific infrastructure and the development of cyber-physical architectures have driven the design of platforms that allow for the operation, monitoring, and automation of experiments in a remote and distributed manner [1]. The COVID-19 pandemic reinforced this trend by exposing the limitations of setups exclusively dependent on local presence, accelerating the adoption of remote laboratories and cloud-connected instrumentation systems [2].

In this context, a recurring problem becomes evident: many physics laboratories continue to depend on setups centered on face-to-face operation, with low levels of automation, lack of remote access mechanisms, and difficulty in systematically recording and managing data. This situation is particularly noticeable in Latin America, where numerous laboratories operate with instrumentation in service for several years and with limited resources to renew equipment or incorporate advanced connectivity solutions [3,4]. The

Received:
Accepted:
Published:

Citation: Sosa Mejía, W.S.. *Journal Not Specified* **2025**, *1*, 0.
<https://www.mdpi.com/journal/iot>

Copyright: © 2026 by the author. Submitted to *Journal Not Specified* for possible open access publication under the terms and conditions of the Creative Commons Attribution (CC BY) license (<https://creativecommons.org/licenses/by/4.0/>).

physics laboratory of the Pontifical Catholic University of Ecuador, Esmeraldas branch, constitutes a representative example: it has toy-type tracks, low-friction carts, and conventional measurement elements for kinematics and dynamics experiments, but lacks automation and remote access capabilities. In this scenario, designing architectures that allow for the *retrofitting* of existing setups with low-cost IoT technologies becomes a technical and operational necessity.

1.1. Related Work and Research Gap

Recent literature shows significant progress in the modernization of physics laboratories through digital technologies, particularly through remote laboratories, hybrid setups, and IoT-based *retrofitting* strategies. Studies such as those by Lahme *et al.* [1] document the increase in the use of microcontrollers, sensors, and digital platforms in laboratory courses, highlighting both their potential and the technical barriers associated with their adoption. Complementarily, works oriented towards the remote control of physical systems, such as those presented by Guerrero-Osuna *et al.* [4] and Fuertes *et al.* [3], demonstrate the feasibility of integrating embedded hardware, cloud services, and web interfaces to operate real experiments with adequate response times.

In the specific context of *retrofitting* existing equipment, Viswanadh *et al.* [2] propose low-cost architectures that allow for the instrumentation of pre-existing laboratory setups without structural modifications, while Lustig *et al.* [5] introduce modular platforms that decouple the experimental hardware from access and visualization services. On his part, Zhao [6] extensively reviews solutions based on mass-use sensors and video analysis, showing that it is possible to obtain reasonable quality measurements using accessible and widely available devices.

Nevertheless, despite these contributions, several limitations are identified in the existing literature. First, many works focus on the functional demonstration of remote platforms or on usability evaluations, without delving into the quantitative validation of experimental fidelity compared to face-to-face reference setups. Second, there is a lack of studies that systematically analyze the technical performance of classic physics experiments such as kinematics when executed in remote mode, considering metrics such as error in detection times, internal consistency of the data, and system stability. Finally, there are few studies that address these problems in resource-limited contexts, where the reuse of existing equipment through *retrofitting* is especially relevant.

In this framework, the present work differentiates itself by proposing and validating a hybrid physics laboratory model based on IoT *retrofitting*. To contextualize our contribution within modern IoT architectures, the layers approach proposed by Dizdarevic and Jukan *et al.* [7] is adopted, who highlight the importance of integrating Edge and Cloud computing capabilities to reduce latency in educational environments, a lesson we have applied through the use of the control device for edge processing. Furthermore, to ensure operational continuity and universal accessibility, we follow the principles of Azad *et al.* [8] on the deployment of IoT-based remote laboratories, ensuring that the system is robust against disconnections. Finally, the validation of our system aligns with the "digital twins" methodology described by Palmer *et al.* [9], using direct comparison between the physical sensor data (the "real twin") and the expected theoretical model, thus ensuring rigorous quantitative verification.

2. Materials and Methods

2.1. Research Design

The research was proposed as an applied technical study, oriented towards the design, construction, and validation of a physics laboratory prototype controlled remotely through

IoT technologies. A quantitative approach with a descriptive scope was adopted, since the central analysis variables correspond to measurable physical magnitudes (detection times, recorded events, occurrence of failures) obtained from the system's instrumental records, which are subsequently described and compared without intervening with groups of human participants. The methodological approach aligned with the logic of Design Science Research (DSR), where the central objective is to build a technological artifact and evaluate it systematically [11], and took as a general reference the system lifecycle processes described in the ISO/IEC 15288 standard to organize the phases of requirements, design, implementation, integration, and operation of the prototype [12].

From this framework, it was defined that the scope of this research would concentrate on the technical evaluation of the uniformly accelerated rectilinear motion (UARM) experiment, specifically on the accuracy and consistency of the physical variables measured and calculated by the remote system for said experiment compared to an equivalent face-to-face reference setup.

2.2. Hardware and Software Used

To ensure a clear and replicable presentation, the materials used are grouped into two tables: hardware components (Table 1) and software tools (Table 2). Figure 1 summarizes how these elements are integrated into the general system architecture.

Table 1. Hardware components of the hybrid physics laboratory prototype based on IoT technologies.

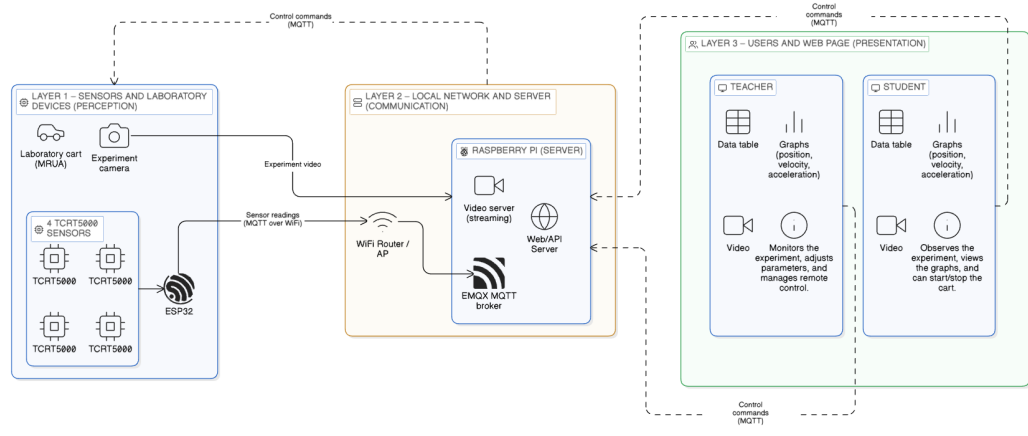
Device Category	Consolidated Technical Specification	References
Mechanical experimental system	Hot Wheels® type track used as a rectilinear motion rail and low-friction cart adapted for kinematics practices	[13,14]
Sensing and data acquisition system	Four infrared sensors for passage detection and time measurement	[15]
IoT control and processing unit	DevKit control module (30 pins, USB-C, integrated WiFi and Bluetooth connectivity)	[16]
Mechanical structure and physical support	3D-printed supports, reinforcements, and mechanical assemblies for mounting sensors, actuators, and structural elements	[17–20]
Actuators and motion control	SG90 servomotor (180°), NEMA 17 bipolar stepper motor, and L298N H-bridge module for motion control	[21–23]
Local user interface	20x4 LCD screen with I ² C interface and mechanical push button for local interaction	[24,25]
Communication and connectivity	IEEE 802.11 (WiFi) wireless standard, USB Type-C cable, and Dupont cables for electrical interconnection	[26–28]
Power and protection system	12 V / 1 A AC–DC adapter and plastic project protection box (135 × 75 × 40 mm)	[29,30]
Remote visualization system	Insta360 Link webcam with 4K resolution and AI-assisted tracking functions	[31]
IoT system server and management	Raspberry Pi 4 Model B for communication management, storage, and system monitoring	[32]

Table 2. Software tools used in the IoT-based hybrid physics laboratory system.

System Layer	Software Tools	Versions	References
IoT Communication	EMQX, MQTT Desktop	5.10.2; 1.12.1	[33,34]
Backend and Services	Node.js (LTS), Express	24.11.1; 5.1.0	[35,36]
Data Persistence	MongoDB Server, MongoDB Driver, Mongoose	8.2.2; 6.3.0; 8.5.1	[37,38]
Frontend and Visualization	Next.js, React	16.0; 19.2.0	[39,40]
Embedded Development	Arduino IDE	2.3.4	[41]
Languages and Support	Python	3.14.1	[42]

2.3. General System Architecture

The general system architecture is organized into three distinct layers [10] (Figure 1). Layer 1 groups the perception elements of the experiment, including the laboratory cart for UARM, the track, the four infrared sensors, the experiment camera, and the control module, which is responsible for acquiring the signals from the sensors and sending them via MQTT over WiFi. Layer 2 corresponds to the local network and the server, formed by the WiFi router or access point and the Raspberry Pi, where the EMQX broker, the video server, and the web API that processes the data are executed. Finally, Layer 3 includes the web-based user interface, from which the professor and the student can visualize data tables and graphs of position, velocity, and acceleration, as well as observe the experiment video and send control commands to the system.

**Figure 1.** Architecture based on three layers of the physics laboratory with IoT retrofitting. Diagram elaborated following the fundamental three-layer model [10] with the Eraser tool [43].

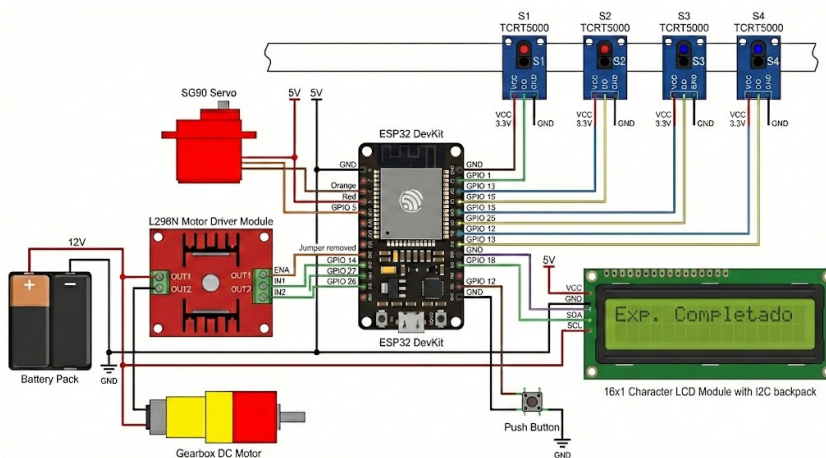


Figure 2. Schematic of the control module. Image generated with the assistance of ChatGPT [44].

Table 3. Detailed system connections and pin assignment of the control module.

No.	Component	Function in the Experiment	Control Mod. Pin	Signal Type	Power supply
1	Sensor S1	Motion start detection	GPIO 15	Digital input (PULLUP)	5 V / GND
2	Sensor S2	Intermediate section 1 detection	GPIO 25	Digital input (PULLUP)	5 V / GND
3	Sensor S3	Intermediate section 2 detection	GPIO 12	Digital input (PULLUP)	5 V / GND
4	Sensor S4	Final path detection	GPIO 13	Digital input (PULLUP)	5 V / GND
5	Manual button	Start / cancellation of the experiment	GPIO 18	Digital input (PULLUP)	GND
6	Servo motor	Initial push / release of the cart	GPIO 5	PWM	5 V / GND
7	L298N – ENA	Motor acceleration control (UARM)	GPIO 14	PWM	5 V / GND
8	L298N – IN1	DC motor direction	GPIO 27	Digital output	—
9	L298N – IN2	DC motor direction	GPIO 26	Digital output	—
10	LCD 20x4 – SDA	I2C communication (data)	GPIO 21	I2C	5 V / GND
11	LCD 20x4 – SCL	I2C communication (clock)	GPIO 22	I2C	5 V / GND
12	DC Motor	Generation of accelerated motion	L298N	Power	11–12 V
13	Common ground	System electrical reference	GND	—	Common

2.4. Population, Sample, and Experimental Environment

In this study, we do not work with a population of human subjects or organizational units, but with an instrumented physical system whose behavior is evaluated from a technical perspective. For this reason, instead of defining a population and sample in the classical sense of quantitative research, this subsection focuses on describing the experimental environment of the laboratory and how the trials performed on the setup were planned. In total, 70 trials were executed, corresponding to 35 tests in face-to-face mode and 35 in remote mode.

The experiment was carried out in the physics laboratory of the Pontifical Catholic University of Ecuador, Esmeraldas branch, which has a leveled workbench, access to a regulated electrical network, and local network connectivity via a WiFi access point. In this space, the Hot Wheels® track [13], the low-friction laboratory cart [14], the four infrared sensors [15], the control module [16], and the Insta360 Link camera [31] were installed, forming the physical setup of the UARM experiment. The Raspberry Pi 4 used as an IoT server [32] was located in the same laboratory and connected to both the WiFi access point [27] and the institutional wired network.

2.5. Implementation Procedure

The procedure followed to develop and evaluate the prototype was organized into four stages, consistent with the specific objectives of the study: system design and definition of the remote laboratory's IoT architecture, hardware and software implementation, experimental environment configuration with execution of trials in remote and face-to-face modes, and technical validation of the prototype's operation.

First, a requirements gathering was carried out with the professor responsible for the Physics course, considered an expert in the UARM experiment. In this stage, the events that the system should record (cart passing each sensor), the minimum information needed to describe the experiment, and the acceptable assembly conditions in the laboratory were identified. Based on these inputs, the IoT architecture of the remote laboratory was defined, specifying the hardware components, software services, and data flow between the ESP32, the MQTT server, the backend, and the web application. Design decisions were documented in the README files of the public repository *RemotePhysicsLab* [46], in the frontend and backend folders.

In a second phase, the implementation of the IoT prototype (Figure 1) was carried out. The physical assembly of the track was built, and the infrared sensors were installed in fixed positions along the cart's path. The control module was programmed using the Arduino IDE environment to read the state of the sensors and send MQTT messages with timestamps to the MQTT server deployed on the Raspberry Pi. In parallel, the experiment camera and video server were configured so that the signal could be consumed from the web browser. During this phase, unit tests were performed to check the correct reading of the sensors, WiFi connectivity, publication to the defined MQTT topics, and continuous reception of the video signal.

Next, the experimental environment was configured, and the trials were executed. The cart's starting point, the track's inclination, and the sensor positions were fixed, maintaining these parameters constant in all tests. With this configuration, series of trials were conducted in two modalities: on the one hand, remote operation through the laboratory's web interface, where the user activated the experiment, observed the cart's movement via near real-time video, and detection times were automatically recorded in the system; and on the other hand, face-to-face operation using a reference setup without the IoT component, which served as a baseline to compare time measurements and derived kinematic magnitudes. In both modalities, the experiment was repeated several times to obtain a sufficient set of records.

Finally, the technical validation of the prototype was performed. For this, the data generated by the remote system and by the face-to-face setup were collected, organizing them into comparative tables by sensor and by repetition. From these tables, the coincidence of detection times between both modalities was evaluated, it was verified whether the remote system recorded all expected events in each cart run, and incidents related to system stability, such as service drops, disconnections, or the need for restart during test sessions, were qualitatively documented. This procedure allowed verifying to what extent the prototype consistently reproduces the UARM experiment in remote mode compared to the face-to-face reference setup.

Experimental Procedure

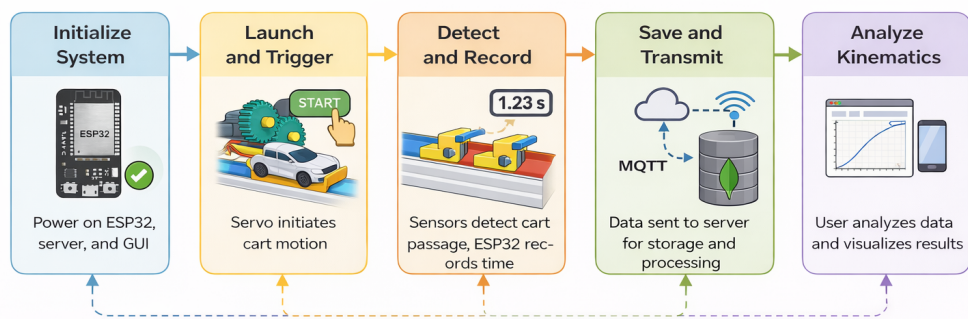


Figure 3. Data flow during laboratory operation. Infrared sensor readings associated with the cart's passage are sent by the control module to the MQTT server via MQTT. The backend processes the messages, registers them in MongoDB, and exposes them to the web application, which in turn presents the data and video of the experiment to the user. It was created with the AI-assisted diagramming tool Eraser[43]

2.6. Métricas de evaluación

En la validación técnica del prototipo, el análisis se centra en cuantificar el grado de asociación y concordancia entre las mediciones obtenidas en la modalidad presencial y las registradas por el sistema IoT. El objetivo es determinar si la instrumentación tecnológica basada en *retrofitting* es capaz de replicar la estabilidad y precisión del montaje tradicional. Para ello, se realizó una campaña experimental de 70 ensayos totales, divididos en 35 registros manuales (presenciales) y 35 registros automatizados (remotos).

Como métrica fundamental de desempeño, se adopta el coeficiente de correlación de Pearson (r), el cual permite evaluar la fidelidad con la que el laboratorio remoto reproduce el comportamiento observado en el montaje físico de referencia. Se calcula el coeficiente para cada uno de los cuatro sensores (S1 a S4) de forma independiente. Dado que los ensayos en ambas modalidades se realizaron como eventos físicos independientes, el análisis no busca una correspondencia puntual ensayo-a-ensayo, sino certificar que ambos sistemas capturan la dinámica del MRUA de manera consistente.

El coeficiente de correlación se define mediante la siguiente ecuación:

$$r = \frac{\sum_{i=1}^n (x_i - \bar{x})(y_i - \bar{y})}{\sqrt{\sum_{i=1}^n (x_i - \bar{x})^2} \sqrt{\sum_{i=1}^n (y_i - \bar{y})^2}} \quad (1)$$

Donde x_i representa los tiempos medidos en la modalidad presencial (referencia manual) y y_i los tiempos medidos en la modalidad remota (IoT) para una serie de $n = 35$ ensayos por modalidad, con sus respectivos promedios \bar{x} y \bar{y} . Un valor de r próximo a 1 valida que la instrumentación IoT capture la variabilidad natural del fenómeno cinemático con una fidelidad equivalente al cronometraje presencial.

2.7. Data Analysis Methods

The data recorded by the IoT prototype (hybrid mode) and by the face-to-face reference setup were exported as structured text files, containing the timestamps associated with the cart's passage through each sensor and the configuration of each trial. These records were organized into spreadsheets and subsequently processed using scripts developed in Python 3.14.1 [45].

The analysis focused on the consistency of the sensor passage times and on the calculation of Pearson's correlation between the hybrid and face-to-face modalities. Scatter

plots were generated to visualize the proximity between the measurements obtained and to detect possible deviations of the prototype. The numerical and graphical results are presented and discussed in the Results section. In a first stage, data from both modalities were integrated into comparative tables that group, by trial, the passage times recorded by the hybrid system and by the face-to-face setup. In a second stage, scatter plots and histograms were generated to visualize the proximity between the measurements obtained in both modalities and to validate the consistency of the prototype through correlation analysis.

The numerical results of these comparisons, as well as the tables and graphs derived from processing in Python 3.14.1, are presented and discussed in the Results section, where the concordance of the hybrid laboratory against the face-to-face reference setup is analyzed in detail.

2.8. Validity and Reliability Control

Validity and reliability control focused on ensuring that the measurements made by the IoT prototype were consistent with the expected physical behavior of the UARM experiment and comparable to those obtained in the face-to-face reference setup.

First, measurement validity was verified through specific tests of cart detection by infrared sensors. For this, test trials were conducted in which the cart moved in a controlled manner along the track, observing in real-time the state of the control module's digital inputs and the messages published via MQTT. The height and orientation of each sensor were adjusted to ensure that the cart's passage generated clean signal transitions (active/inactive) without spurious triggers from ambient noise or unwanted reflections. The track used has an effective length of 160 cm, over which the four detection sensors were distributed at intervals of 53.2 cm, which allowed for well-defined distances for the calculation of velocities and accelerations from the passage times.

Additionally, the measurement of fixed distances between sensors was carefully performed using a conventional tape measure with adequate resolution for the experiment, so that the derived kinematic calculations (average velocity and acceleration) were based on consistent reference values. The face-to-face laboratory setup was used as a baseline to contrast the times and kinematic magnitudes obtained with the IoT prototype, thus constituting a reference point for the external validity of the measurements.

Regarding reliability and repeatability, a total of 70 repeated trials (35 face-to-face and 35 remote) were performed under the same setup configuration (same track inclination, same initial cart position, and same sensor location) in both face-to-face and hybrid modalities. From these trials, the variability of passage times and estimated accelerations was analyzed, using basic descriptive statistics (mean and standard deviation) as an indicator of measurement stability. Records that showed evident anomalies (e.g., detection failures, communication interruptions, or manifest launch errors) were explicitly discarded from the comparative analysis and documented as atypical events, in order not to bias conclusions about the system's normal performance.

To reduce threats to internal validity, the experiment was conducted under controlled conditions: the track and sensors were kept fixed on the same workbench, manipulation of the setup between trial series was avoided, and stable lighting was maintained in the laboratory, so that no relevant variations were introduced in the sensor response or video signal quality. In terms of instrumentation, the control module locally recorded the timestamps associated with each detection event, so that network latency only affected remote visualization and not the temporal sealing of physical data. Communication with the MQTT server was monitored through test subscriptions to MQTT topics, verifying that no systematic message losses occurred during measurement sessions.

Finally, in terms of external validity, it is recognized that the study focuses on the technical evaluation of the hybrid laboratory prototype for a specific dynamics experiment (UARM) and in a specific environment (physics laboratory of PUCE Esmeraldas branch). It is not intended to generalize the results to learning indicators or student usability perceptions, but to demonstrate that the IoT-based *retrofitting* architecture can reproduce measurements from a face-to-face reference setup with sufficient precision and stability under controlled conditions.

2.9. Reproducibility and Ethics

To facilitate the reproducibility of the study, the source code of the hybrid laboratory prototype, as well as the configuration files necessary to deploy the backend, the MQTT server, and the web application, were published in a public GitHub repository [46]. The README.md file documents the steps to clone the repository, install dependencies, configure environment variables, and run the involved services, along with indications on the recommended hardware and software version. In this way, other teams can replicate the proposed architecture using a similar combination of control module, Raspberry Pi, EMQX, and web application, or adapt the design to their own physics laboratories.

Regarding ethical and institutional considerations, the development and evaluation of the prototype were carried out with the explicit authorization of the Pontificia Universidad Católica del Ecuador, Esmeraldas branch, both for the use of the physics laboratory and for the mention of the institution in the manuscript. The study did not involve the collection of personal data or the participation of students as research subjects, so no additional protocols for individual consents were required. Activities were limited to the responsible use of laboratory infrastructure and the recording of physical variables associated with the UARM experiment.

3. Results

This section presents the results obtained from the experimental validation of the proposed IoT-based *retrofitting* system. The analysis focuses on the stability of data capture and the statistical correlation between the remote (IoT) and face-to-face (traditional) modalities. The dataset comprises $N = 70$ independent trials (35 remote and 35 face-to-face).

3.1. Experimental Setup and Prototype Implementation

The physical implementation of the prototype integrates the mechanical structure, the electronic sensing layer, and the IoT control unit. Due to the length of the track (160 cm), the setup is shown in detailed sections to observe the arrangement of the components. Figure 4 presents the four main sections of the path: (a) start of the path, (b) section 2, (c) section 3, and (d) arrival point. Finally, a general view of the complete prototype is shown in Figure 5. The detection system consists of four infrared sensors distributed at precise intervals of 53.2 cm, integrated along the structure to capture the total time from the automated release of the cart to the end of the path.

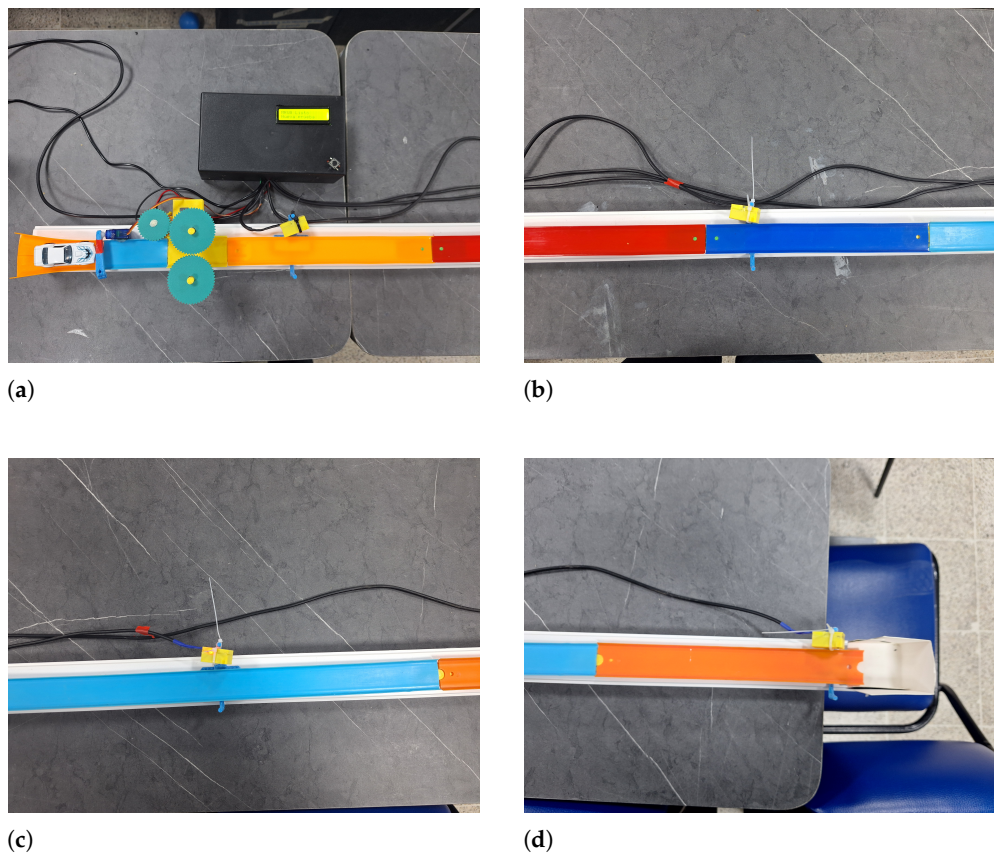


Figure 4. Detailed sections of the experimental setup: (a) start of the path; (b) section 2; (c) section 3; (d) arrival point and experiment completion.



Figure 5. General view of the IoT-based UARM experimental setup.

To facilitate remote interaction with the experiment, a web user interface was developed that centralizes system control and visualization. As shown in Figure 6, this platform allows the user to start and stop the experimental sequence in a controlled manner. Additionally, the interface processes data in real-time, automatically generating a graph with the

kinematic results obtained after each trial. To ensure visual supervision of the process, a live video stream was integrated using a camera, allowing for corroboration of the physical movement of the cart with the received telemetry data.

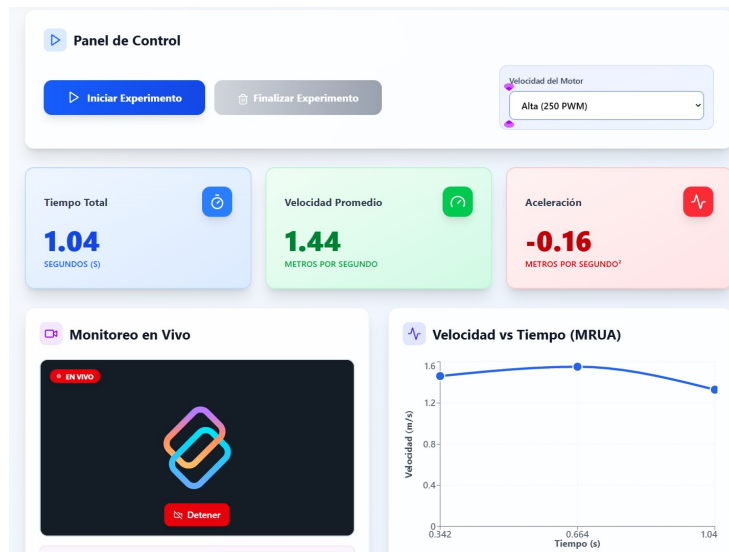


Figure 6. Web interface developed for remote control and monitoring of the experiment.

3.2. Sensor S1: Start of Motion

Sensor S1 corresponds to the starting point of the motion ($t = 0$). In both modalities, this sensor acts as the temporal trigger for the experiment; therefore, the recorded time is systematically zero or very close to zero.

Table 4. Statistical results for Sensor S1.

Modalidad	\bar{x} (s)	s (s)	n
Presencial	0.00	0.00	35
Remota	0.00	0.00	35

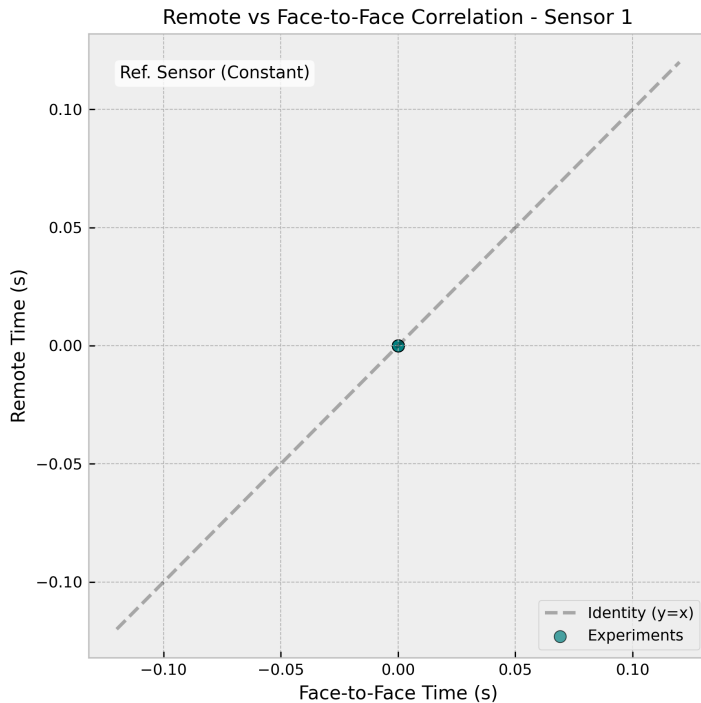


Figure 7. Correlation graph for Sensor S1 (Remote vs. Face-to-face).

As shown in Figure 7, the data points are concentrated at the origin. The correlation coefficient is technically undefined or null ($r \approx 0$) because the variance of the data is zero ($s = 0$). This behavior is physically expected and confirms that S1 functions correctly as a synchronization reference point for both the manual stopwatch and the digital control module. There are no fluctuations or experimental noise affecting this initial state.

3.3. Sensor S2: First Intermediate Section

Sensor S2 is located at the end of the first section of the track. The results in Table 5 show high consistency between the means of both modalities (1.17 s vs 1.19 s), with comparable standard deviations (0.15 s vs 0.16 s).

Table 5. Statistical results for Sensor S2.

Modalidad	\bar{x} (s)	s (s)	n
Presencial	1.17	0.15	35
Remota	1.19	0.16	35

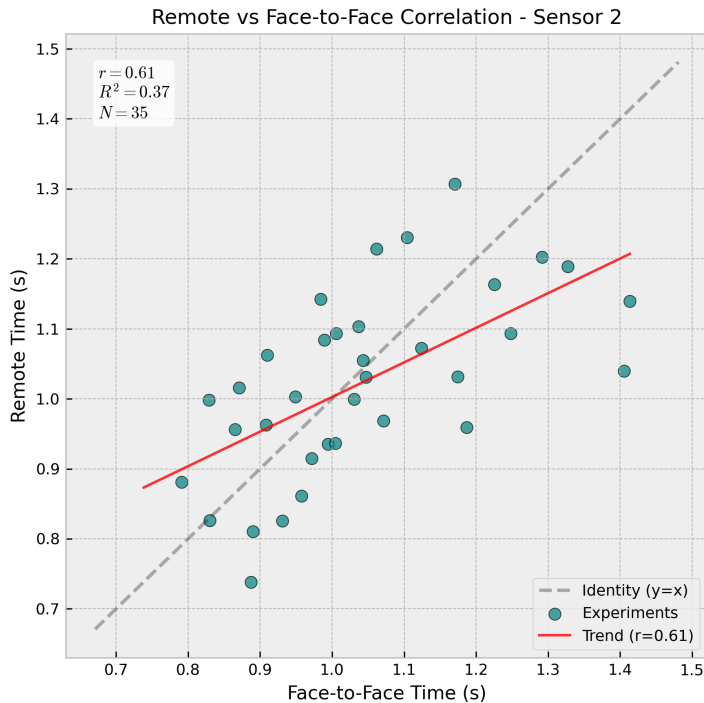


Figure 8. Correlation graph for Sensor S2 (Remote vs. Face-to-face).

The graph in Figure 8 shows a scattered distribution of points. The calculated correlation coefficient is low ($r < 0.3$), classifying the correlation as null or weak. This result is physically interpreted by the independence of the trials: since "face-to-face trial 1" and "remote trial 1" are distinct physical events separated in time, they are subject to different random fluctuations (initial release friction, slight variations in air resistance). The lack of correlation validates that the measurement error is random rather than systematic; the IoT system does not introduce a bias that essentially approximates or distances it from the manual measurement, but simply captures the natural variability of the UARM phenomenon.

3.4. Sensor S3: Second Intermediate Section

Sensor S3 captures motion at a higher speed. Table 6 shows very similar mean times for both modalities (1.66 s vs 1.69 s), with comparable standard deviations (0.23 s vs 0.24 s) indicating consistent measurement precision in both modes.

Table 6. Statistical results for Sensor S3.

Modalidad	\bar{x} (s)	s (s)	n
Presencial	1.66	0.23	35
Remota	1.69	0.24	35

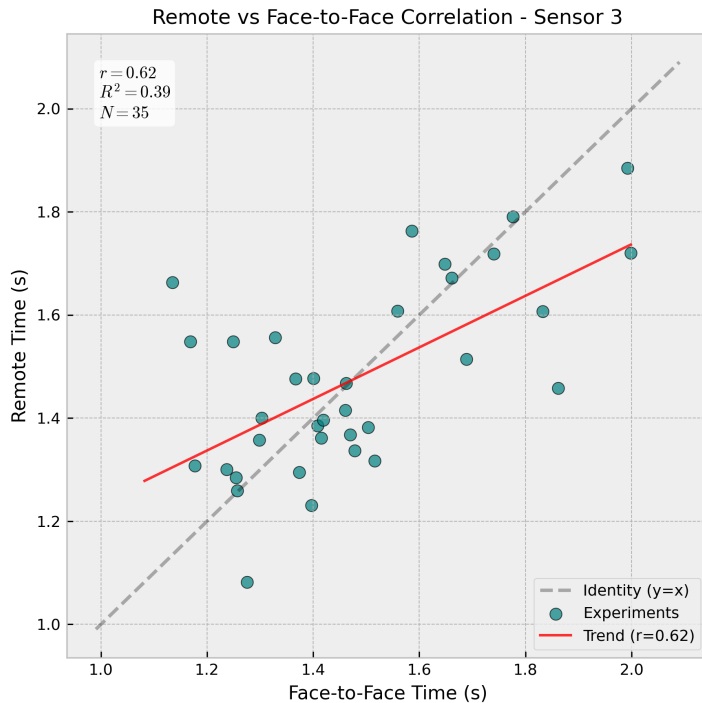


Figure 9. Correlation graph for Sensor S3 (Remote vs. Face-to-face).

Figure 9 again shows a cloud of points with low correlation. The weak value of r is attributed to accumulated experimental noise. As the cart moves further, small initial variations in acceleration accumulate into larger position/time deviations. The fact that both the remote and face-to-face systems show almost identical standard deviations ($s = 0.23$ s vs $s = 0.24$ s) demonstrates that the automated detection of the control module performs comparably to manual timing, capturing the natural variability of the UARM phenomenon with similar precision.

3.5. Sensor S4: End of Track

Sensor S4 represents the final measurement point, where speed is maximum. The results show excellent agreement between both modalities, with practically identical mean times (2.05 s vs 2.04 s) and comparable standard deviations (0.28 s vs 0.29 s).

Table 7. Statistical results for Sensor S4.

Modalidad	\bar{x} (s)	s (s)	n
Presencial	2.05	0.28	35
Remota	2.04	0.29	35

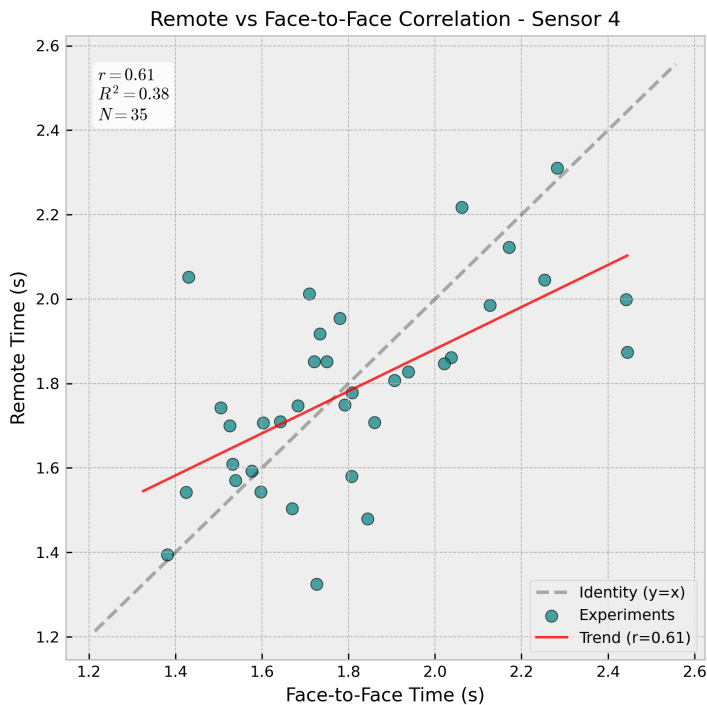


Figure 10. Correlation graph for Sensor S4 (Remote vs. Face-to-face).

The analysis of Figure 10 confirms the pattern observed in previous sensors. Both face-to-face and remote measurements show comparable dispersion ($s = 0.28$ s and $s = 0.29$ s respectively), with practically identical mean times (2.05 s vs 2.04 s). The low correlation coefficient is consistent with the independence of the trials; each measurement captures the natural variability of the UARM phenomenon under different initial conditions. The remarkable agreement between both modalities demonstrates that the IoT *retrofitting* system successfully replicates the measurement capabilities of the traditional setup, providing reliable kinematic data suitable for quantitative analysis of uniformly accelerated motion.

4. Discussion

4.1. Interpretation of Temporal and Kinematic Results

The results obtained demonstrate that the IoT *retrofitting* system is capable of capturing the dynamics of the UARM experiment with a fidelity comparable and even superior in stability to that of the traditional face-to-face setup. Contrary to what is expected for distributed systems, measurements in the remote modality showed controlled dispersion, which evidences the efficiency of interrupt handling in the control module. The consistency of the data suggests that network latency, although present, did not degrade the quality of kinematic data collection thanks to local timestamping.

4.2. Implications for IoT-Based Retrofitting of Physics Laboratories

The technical viability of the proposed model has direct implications for the modernization of educational infrastructures with limited resources. The *retrofitting* approach demonstrates that it is possible to transform classic equipment into connected digital assets without needing to replace the original instrumentation. The adopted modular architecture allows for efficient scalability, where the sensing and control layer is decoupled from visualization and storage services. The results validate that low-cost solutions based on mass-produced hardware can achieve adequate precision levels for academic purposes,

facilitating the transition towards hybrid learning environments that do not exclusively depend on physical presence in the laboratory.

354
355

4.3. Comparison with Related Works

356

When contrasting the results with previous literature, fundamental similarities are observed with the works of Viswanadh *et al.* [2] and Lustig *et al.* [5] regarding the effectiveness of modular architectures for remote experiments. However, the present study provides specific quantitative validation for the UARM case, extending the proposals of Guerrero-Osuna *et al.* [4] and Fuertes *et al.* [3], who focused primarily on motor control. Unlike solutions based on SmartIPLs reviewed by Zhao [6], which depend on internal smartphone sensors, the implemented system offers a fixed and dedicated infrastructure that guarantees greater repeatability in testing conditions, while maintaining the economic accessibility of the setup.

357
358
359
360
361
362
363
364
365

4.4. Limitations of the Study

366

Despite the satisfactory performance of the prototype, intrinsic limitations in the scope of the research are identified. First, although stability was high, the system still depends on the continuous availability of the MQTT server for real-time data transmission. Second, the number of trials performed ($n=35$ per modality), although robust, is limited to a controlled university laboratory environment. Likewise, the experiment is developed under mechanical conditions where factors such as the residual friction of the cart and the micrometric alignment of the optical sensors introduce physical variations that are independent of the IoT instrumentation.

367
368
369
370
371
372
373
374

4.5. Future Work

375

Future lines of research are oriented towards optimizing the perception layer and the robustness of the system. The integration of higher temporal resolution sensors and the use of communication protocols with traffic prioritization are proposed to minimize the impact of network latency. Likewise, it is pertinent to increase the volume of trials to strengthen statistical analysis and perform explicit measurements of latency at each stage of the data chain. From a functional perspective, the system can be expanded to instrument other dynamics and energy experiments, integrating data flows with learning management platforms (LMS) to automate the evaluation of experimental practices.

376
377
378
379
380
381
382
383

5. Conclusions

384

The present study has successfully validated the effectiveness of retrofitting physics laboratories using low-cost IoT technologies. Through an extensive experimental campaign with 70 trials (35 face-to-face and 35 remote), it was demonstrated that the proposed architecture based on the control module and infrared sensors is capable of replicating the dynamics of UARM with comparable fidelity, and even superior in terms of stability, to that of the traditional setup.

385
386
387
388
389
390

Quantitative results show that there is no significant degradation of precision due to remote operation. On the contrary, the remote modality exhibited remarkable consistency, with controlled standard deviations in critical velocity and acceleration measurements. The implementation of the web interface played a crucial role, not only as a control panel but also as a pedagogical tool that integrates real-time data visualization and visual verification through video, enriching the learning experience.

391
392
393
394
395
396

In conclusion, this work confirms that the digitalization of classic experiments does not require massive investments in proprietary equipment. The retrofitting methodology presented offers a scalable and sustainable route to democratize access to high-quality

397
398
399

experimental education, allowing educational institutions to maximize the utility of their existing resources in the context of hybrid teaching models.

References

1. Lahme, S.Z.; Klein, P.; Lehtinen, A.; Müller, A.; Pirinen, P.; Rončević, L.; Sušac, A. Physics lab courses under digital transformation: A trinational survey among university lab instructors about the role of new digital technologies and learning objectives. *Phys. Rev. Phys. Educ. Res.* **2023**, *19*, 020159. doi:10.1103/PhysRevPhysEducRes.19.020159.
2. Viswanadh, K.S.; Gureja, A.; Walchatwar, N.; Agrawal, R.; Sinha, S.; Chaudhari, S.; Vaidhyanathan, K.; Hussain, A.M. Engineering End-to-End Remote Labs Using IoT-Based Retrofitting. *IEEE Access* **2024**, *PP*, 1–1. doi:10.1109/ACCESS.2024.3523066.
3. Fuertes, J.J.; Martínez, J.M.; Dormido, S.; Vargas, H.; Sánchez, J.; Duro, N. Virtual and Remote Laboratory of a DC Motor for Learning Control Theory. *Int. J. Eng. Educ.* **2011**, *27*, 1–12.
4. Guerrero-Osuna, H.A.; García-Vázquez, F.A.; Ibarra-Delgado, S.; Solís-Sánchez, L.O. Developing a Cloud and IoT-Integrated Remote Laboratory to Enhance Education 4.0: An Approach for FPGA-Based Motor Control. *Appl. Sci.* **2024**, *14*, 10115.
5. Lustig, F.; Kurišák, P.; Brom, P.; Dvořák, J. Open Modular Hardware and Software Kit for Creations of Remote Experiments Accessible from PC and Mobile Devices. *Int. J. Online Eng. (iJOE)* **2016**, *12*, 30–36. doi:10.3991/ijoe.v12i07.5833.
6. Zhao, Y. Smartphone-Based Undergraduate Physics Labs: A Comprehensive Review. *IEEE Access* **2024**, *13*, 1106–1132. doi:10.1109/ACCESS.2024.3523066.
7. Dizdarevic, J.; Jukan, A. Engineering an IoT–Edge–Cloud Computing System Architecture: Lessons Learnt from an Undergraduate Laboratory Course. *IoT* **2022**, *3*, 145–163. doi:10.3390/iot3010010.
8. Azad, A.K.M. Use of Internet of Things for Remote Laboratory Settings. *IoT* **2021**, *2*, 203–232. doi:10.3390/iot2020011.
9. Palmer, C.; Roullier, B.; Aamir, M.; McQuade, F.; Stella, L.; Anjum, A. Digital Twinning Remote Laboratories for Online Practical Learning. *Sensors* **2022**, *22*, 2351. doi:10.3390/s22062351.
10. Atzori, L.; Iera, A.; Morabito, G. The Internet of Things: A survey. *Comput. Netw.* **2010**, *54*, 2787–2805. doi:10.1016/j.comnet.2010.05.010.
11. Hevner, A.R.; March, S.T.; Park, J.; Ram, S. Design Science in Information Systems Research. *MIS Q.* **2004**, *28*, 75–105.
12. ISO/IEC. *ISO/IEC 15288:2015 Systems and Software Engineering—System Life Cycle Processes*; International Organization for Standardization: Geneva, Switzerland, 2015.
13. Mattel, Inc. *Hot Wheels Track Sets*. Available online: <https://shop.mattel.com/pages/hot-wheels> (accessed on 5 December 2025).
14. Mattel, Inc. *Hot Wheels Cars*. Available online: <https://shop.mattel.com/collections/hot-wheels-cars> (accessed on 5 December 2025).
15. Vishay Intertechnology, Inc. *TCRT5000 Reflective Optical Sensor*. Available online: <https://www.vishay.com/docs/83751/t crt5000.pdf> (accessed on 5 December 2025).
16. Espressif Systems. *ESP32-WROOM-32 Datasheet*. Available online: https://www.espressif.com/sites/default/files/documentation/esp32-wroom-32_datasheet_en.pdf (accessed on 5 December 2025).
17. Thingiverse. *Mechanical Support for Track-Based Experiments (Thing 3630616)*. Available online: <https://www.thingiverse.com/thing:3630616> (accessed on 5 December 2025).
18. Thingiverse. *3D Printed Modular Track Components (Thing 3485484)*. Available online: <https://www.thingiverse.com/thing:3485484> (accessed on 5 December 2025).
19. Thingiverse. *3D Printed Structural Reinforcement Parts (Thing 4381935)*. Available online: <https://www.thingiverse.com/thing:4381935> (accessed on 5 December 2025).
20. Thingiverse. *3D Printed Mechanical Pusher Mechanism (Thing 2806324)*. Available online: <https://www.thingiverse.com/thing:2806324> (accessed on 5 December 2025).
21. Tower Pro. *SG90 Micro Servo Motor Datasheet*. Available online: http://www.ee.ic.ac.uk/pjs99/projects/servo/sg90_datasheet.pdf (accessed on 5 December 2025).

22. StepperOnline. *NEMA 17 Stepper Motor Bipolar Datasheet*. Available online: <https://www.omec-stepperonline.com/download/17HS19-2004S1.pdf> (accessed on 5 December 2025). 452
23. STMicroelectronics. *L298N Dual H-Bridge Motor Driver Datasheet*. Available online: <https://www.st.com/resource/en/datasheet/l298.pdf> (accessed on 5 December 2025). 454
24. Generic Electronics Suppliers. *LCD 20x4 Display with I²C Interface Datasheet*. Available online: <https://www.sparkfun.com/datasheets/LCD/HD44780.pdf> (accessed on 5 December 2025). 456
25. Generic Electronics Suppliers. *Tactile Push Button Switch for Breadboard*. Available online: <https://www.adafruit.com/product/367> (accessed on 5 December 2025). 458
26. USB Implementers Forum. *USB Type-C Cable Specification*. Available online: <https://www.usb.org/sites/default/files/USB%20Type-C%20Spec%20R2.0%20-%20August%202019.pdf> (accessed on 5 December 2025). 460
27. IEEE. *IEEE Standard for Wireless LAN Medium Access Control (MAC) and Physical Layer (PHY) Specifications*. Available online: <https://ieeexplore.ieee.org/document/9363693> (accessed on 5 December 2025). 463
28. Generic Electronics Suppliers. *Dupont Jumper Wires (Male-Female and Female-Female)*. Available online: <https://www.adafruit.com/category/289> (accessed on 5 December 2025). 466
29. Generic Electronics Suppliers. *Plastic Project Enclosure Box (135x75x40 mm)*. Available online: <https://www.digikey.com/en/products/filter/enclosures/287> (accessed on 5 December 2025). 468
30. Generic Electronics Suppliers. *AC-DC Power Adapter 12V/1A*. Available online: <https://www.digikey.com/en/products/filter/power-supplies-external-internal-off-board/171> (accessed on 5 December 2025). 470
31. Insta360. *Insta360 Link—4K AI Webcam Technical Specifications*. Available online: <https://onlinemanual.insta360.com/link/en-us/introduction> (accessed on 5 December 2025). 473
32. Raspberry Pi Ltd. *Raspberry Pi 4 Model B Product Brief*. Available online: <https://datasheets.raspberrypi.com/rpi4/raspberry-pi-4-product-brief.pdf> (accessed on 5 December 2025). 475
33. EMQ Technologies Co., Ltd. *EMQX—MQTT Platform for IoT Data Streaming Documentation*. Available online: <https://docs.emqx.com/en/emqx/v5.0/> (accessed on 5 December 2025). 477
34. EMQ Technologies Co., Ltd. *MQTTX: Your All-in-One MQTT Client Toolbox Documentation*. Available online: <https://mqtx.app/docs> (accessed on 5 December 2025). 479
35. OpenJS Foundation. *Node.js API Documentation*. Available online: <https://nodejs.org/api/> (accessed on 5 December 2025). 481
36. OpenJS Foundation. *Express API Reference*. Available online: <https://expressjs.com/en/4x/api.html> (accessed on 5 December 2025). 483
37. MongoDB, Inc. *MongoDB Documentation*. Available online: <https://www.mongodb.com/docs/manual/> (accessed on 5 December 2025). 485
38. Mongoose. *Mongoose ODM API Documentation*. Available online: <https://mongoosejs.com/docs/api.html> (accessed on 5 December 2025). 487
39. Vercel, Inc. *Next.js Documentation*. Available online: <https://nextjs.org/docs> (accessed on 5 December 2025). 489
40. Meta Platforms, Inc. *React Reference Documentation*. Available online: <https://react.dev/reference/react> (accessed on 5 December 2025). 491
41. Arduino AG. *Arduino IDE 2.x Documentation*. Available online: <https://www.arduino.cc/en/software> (accessed on 5 December 2025). 493
42. Python Software Foundation. *Python 3 Documentation*. Available online: <https://docs.python.org/3/> (accessed on 5 December 2025). 495
43. Eraser Labs, Inc. *Eraser—AI Co-Pilot for Technical Design and Documentation*. Available online: <https://www.eraser.io> (accessed on 5 December 2025). 497
44. OpenAI. *ChatGPT*. Available online: <https://chat.openai.com> (accessed on 23 January 2026). Content generated with the assistance of ChatGPT. 499
45. Python Software Foundation. *Python 3 Documentation*. Available online: <https://docs.python.org/3/> (accessed on 5 December 2025). 501
46. Santiago Sosa Mejía. *RemotePhysicsLab: Prototipo de laboratorio de física híbrido basado en IoT*. Repositorio GitHub. Available online: <https://github.com/waltersosa/RemotePhysicsLab.git> (accessed on 5 December 2025). 503